The Structural Spatial Potential of Myanmar's Trade Network, 1948–2025: A Geospatial Quantum-Optimization Approach

Thu Maung Zaw
School of Management, Mae Fah Luang University
6631202105@lamduan.mfu.ac.th

Received July 12, 2026
Revised September 27, 2026
Accepted October 1, 2026

Abstract

Archival trade statistics for Myanmar are limited. This paper builds a model of the country's trade network that needs none of them. It uses only open geospatial data. The inputs are city coordinates, terrain measured from a public elevation model, and the documented opening dates of transport corridors. From these, the paper computes the pattern of possible trade imposed by geography and the technology of each period. The optimisation problem is written as a division of the corridor network into two groups. Every instance is solved exactly by classical enumeration. The same problem is also given to a quantum algorithm, which is reported strictly as a methodological benchmark. Three findings follow for 1948 to 2025. First, the division of the network is the same in every period. It also survives every alternative setting of the model's five conventions but one. That exception removes the very distinction the study measures. Infrastructure has therefore raised how much a fixed structure can carry without changing the structure. Second, capacity grew by about 28 per cent in two dated steps. Of that growth, 98.9 per cent fell on corridors that link the two groups rather than on corridors inside them. The towns bypassed by the 2010 expressway lost about a third of their network weight. Third, physical friction is separate from realized trade flows.

Keywords: economic geography; transport corridors; spatial structure; infrastructure; Myanmar
JEL Classification Codes: C61, C63, N75, O18, R12

1. Introduction

The spatial structure of an economy is the pattern of which places exchange with which. Economists normally recover that pattern from trade quantities. For many developing economies, those quantities are not usable at the level required. Customs series are limited. Myanmar between 1948 and 2025 is a clear case. The statistics of the decades are limited for trade capacity across towns (Brown, 2013; Myint, 2008). Bilateral totals with partner countries do survive in international collections. No database reports the flow between Mandalay and Muse, or between Yangon and Pathein. Those town-to-town links are the object of this paper.

The paper therefore works from inputs that survive for any country and any period. The importance of a place is computed from the transport network itself. The intensity of a corridor comes from a gravity model. Its friction terms are measured from a public elevation model rather than assumed. Technology enters through multipliers attached to corridor layers with documented opening dates.

What the model measures is not realized trade. It is structural spatial potential. This is the pattern of exchange that the map and the technology of a period make best. The question comes from Findlay's studies. He wrote in Rangoon at the start of the interval studied here. Findlay (1962) treated the allocation problem of a developing economy as a sequence of decisions. He asked what structure mathematics makes best, and how that best structure moves over time. This paper asks the same question in space rather than across sectors. Two differences matter, and both limit what may be claimed. Findlay's problem runs through time. The design here solves five separate static network problems, one for each infrastructure period, and compares the answers. There is no path between periods. The second difference is sharper. The two groups the model produces are a division of places, not of activities. They are not Findlay's agriculture and industry division. Findlay inspires the question. His model is not implemented here. The question is this. In an economy, whose historical trade data cannot be used, how do geography and changing transport technology determine the optimal structure of exchange? And how far does that structure respond to new infrastructure over time?

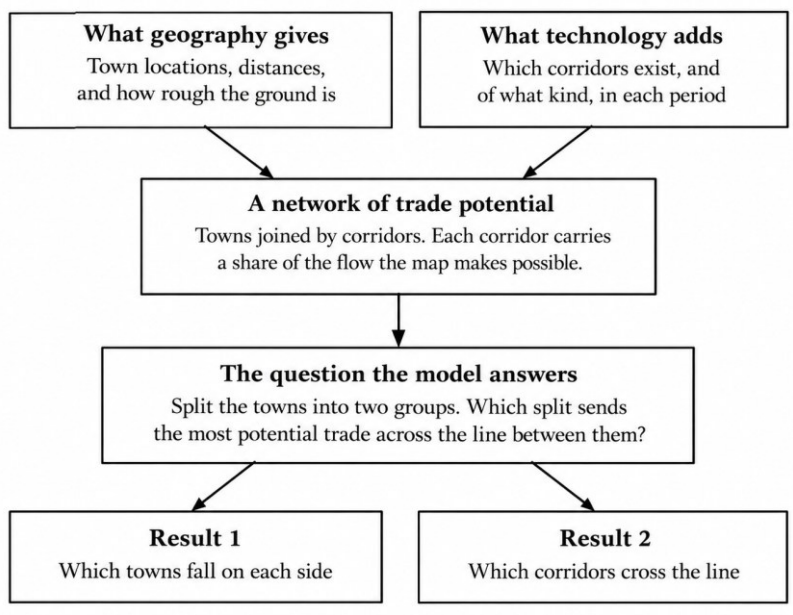

Source: Author constructed.

Figure 1. The conceptual framework.

The paper contributes in three ways. The first is conceptual. It builds a measure of structural spatial potential for a setting where trade volumes are missing. It also states exactly what that measure identifies. The measure gives the membership of a two-group division and the corridors that cross it. It does not give a meaningful scalar level. The second is methodological. The paper connects measured geospatial friction to optimization over network divisions. Every instance is checked against exact enumeration. The third is empirical. The paper reconstructs seventy-seven years of Myanmar's structural geography. It reports which features are stable across model settings and which are not.

The paper is organized as follows. Section 2 reviews previous studies. Section 3 describes the data and methodology. Section 4 reports the results and discusses the findings. Section 5 states the limitations. Section 6 concludes with recommendations.

2. Literature Review

2.1 Trade geography in data-scarce economies

Where trade quantities exist, the gravity model has organised their analysis since Tinbergen (1962). Interaction rises with the product of two masses and falls with the separation between them. Quantitative geography then refined the separation term into a friction of distance. Terrain, mode and infrastructure together set the effective cost of a kilometre (Hansen, 1959; Rodrigue, 2020).

That transport costs matter for trade and income is well established. Limao and Venables (2001) estimate how trade responds to transport cost. Gallup, Sachs and Mellinger (1999) document the link between physical geography and income levels.

Where quantities do not exist, the usual step is to approximate potential from the map. A gravity model combined with measures of network position gives the interaction structure of an economy from geography alone. That is what recommends the approach here. The importance of a node follows the centrality tradition of Freeman (1977) and is computed with the algorithm of Brandes (2001).

2.2 Network partitioning and spatial economics

The claim that geography fixes trade structure over long periods is not new. Peschel (1985) studied Western Europe and North America between 1900 and 1975. She found the countries grouped almost identically in both years. Bilateral trade values correlated above 0.82 across the interval. She concluded that a natural spatial ordering exists, and that political factors weaken it without overturning it. The idea is older still. Predöhl (1949/1971, as cited in Peschel, 1985) held that two groups of factors govern the spatial order of the world economy. Economic forces establish a natural ordering. Political factors may change it but not overturn it. That is the same distinction this paper draws between structure and realisation. Both earlier accounts rest on bilateral trade statistics. The question here is whether the same can be shown without them.

The methods differ in a way that is easy to miss. Peschel's integration areas come from clustering. Clustering groups strongly trading places together. The division used here comes from a graph cut. A cut places strongly linked nodes on opposite sides. The two constructions are opposites. The economic case for the cut is straightforward. It identifies the line across which the geography and technology of a period send the most potential flow. That is a boundary of maximum exchange. It is the spatial counterpart of a trade boundary, not of a region.

2.3 Infrastructure and growth in Southeast Asia

Whether building roads raises long-run income is contested. Aschauer (1989) opened the modern debate on public capital. Donaldson (2018) and Donaldson and Hornbeck (2016) find large effects for colonial Indian railways and for American market

access. Banerjee, Duflo and Qian (2020) find more modest ones for China. Redding and Turner (2015) survey the field. The regional context for Myanmar appears in the Greater Mekong Subregion literature (Krongkaew, 2004; Ishida, 2013; Asian Development Bank, 2018), which also supplies corridor definitions and upgrading dates.

This paper does not enter that debate on its own terms. It contains no realised output that can be attributed to corridors. It occupies the position before that debate. What capacity did the physical network make available, and how did that capacity change? Treating the object as potential rather than outcome keeps the two questions apart. Section 4.3 shows why the separation matters.

3. Data and Methodology

3.1 Data selection and period snapshots

The network is a graph (G). Its node set is fixed. Its corridor set changes by period.

$$G_t = (V, E_t) \quad (1)$$

where V is the fixed node set, of size eighteen; E is the set of corridors active in year t.

The node set holds fifteen Myanmar trade centres and three external market anchors. Cities were chosen on three stated criteria. Each appears as a named trade centre in the historical literature. Each sits on a documented long-distance corridor. And together they cover every major sub-region, so that the river spine, the delta, the coastal arc, the dry zone and both land frontiers are represented.

A coordinate enters both the distance and the terrain profile. What it denotes is therefore part of the model. City nodes are the modern urban centroid. The border nodes Muse and Myawaddy are the crossing point. The port nodes Yangon, Pathein, Mawlamyine and Sittwe are the historic river or estuary port. Appendix Table A1 is the full register.

The three anchors stand for the external markets in which Myanmar corridors end. Kunming stands for Yunnan and China. Bangkok stands for Thailand and mainland Southeast Asia. A maritime node stands for world trade through the Bay of Bengal. That node is a notional waypoint south of the delta, at 14.000 degrees north and 95.000 degrees east. It is included so that the four ports face an outside mass. Without it they would be dead ends rather than gateways. Its position is not a claim about any particular shipping route. Appendix Table C4 reports that moving it by up to two degrees, or removing it altogether, leaves the division of the remaining nodes unchanged.

Twenty-three physical corridors carry thirty-two dated technology layers. Each entry records endpoints, mode and dates, and nothing else (Appendix Table A2). The model is evaluated at 1948, 1970, 1990, 2010 and 2025. The gaps between those years are uneven for a reason. The years are not a sample from a continuous process. Solving the model for every year from 1948 to 2025 gives only three distinct corridor configurations. The five modelled years therefore cover all the variation this design can detect. Every result is a comparison between regimes, not a time series. Two milestones separate the three regimes. The first is the rebuilding of the border highways to the Chinese and Thai frontiers around 1990. The second is the Yangon to Naypyidaw to Mandalay expressway around 2010, together with the upgraded Asian Highway route and the Chinese expressway network reaching the northern border. No corridor in the register opens between 1949 and 1989.

3.2 Network friction and node mass

Distances are geodesics on the World Geodetic System 1984 ellipsoid. Terrain is measured, not assumed. Each corridor is sampled at thirteen points against a ninety-metre elevation model (Farr et al., 2007). Ruggedness is the total rise and fall along the route, divided by its length.

$$r_{ij} = \left(\sum_{k=1}^{12} |h_{k+1} - h_k|\right) / d_{ij} \quad (2)$$

where r_{ij} is ruggedness, in metres of relief per kilometre of route; h_k is elevation in metres at the k-th of thirteen sample points; d_{ij} is the geodesic distance in kilometres.

$$f_{ij} = 1 + r_{ij}/10 \quad (3)$$

where f_{ij} is the friction multiplier. It has no units and is at least one; the divisor 10 is in metres per kilometre. It is a scale, not an estimated parameter. A corridor that climbs ten metres for every kilometre gets exactly twice the friction of a flat one. Across this network f runs from 1.000 to 2.139. The highest value is the Shan Plateau crossing from Mandalay to Muse. Each technology layer carries a mode multiplier. River, coastal and sea links take three. Unimproved road takes four. Rail takes ten, highway twelve and expressway fifteen. The travel cost of a corridor is distance times friction, divided by the multiplier, taking the best layer active in that period. Betweenness centrality is computed on that cost. Shortest paths therefore already reflect terrain and technology.

The mode multiplier therefore enters the model in two places. It sets the travel cost used for betweenness. It also scales the corridor weight in Equation (6). This is deliberate, not an oversight. A better mode raises two different things. It raises the transit role of a node, because more least-cost paths run through it. It also raises the capacity of the corridor itself. Both effects are real and they are separate. Section 4.1 reports what happens when the multiplier is taken out of the cost metric and left only in the weight.

Node mass combines transit position with simple connectivity and with physical endowment.

$$v_{i,t} = g_i \left(1 + k_{i,t}\right)\left(1 + 4b_{i,t}\right) \quad (4)$$

where $v_{i,t}$ is the mass of node i in period t, in index units; $k_{i,t}$ is the degree of node i, and b(i,t) its normalised weighted betweenness centrality (Brandes, 2001); g_i is the physical endowment factor. It multiplies 1.5 for delta or alluvial arable land, 1.5 for onshore oil geology and 1.25 for a natural harbour; external anchors take the fixed mass $v = 12$ instead.

Corridor weight is a gravity term. It uses the two masses, exponential distance decay and measured friction. Parallel modes on one corridor are added, because they add capacity.

$$w_{ij,t} = \sum_{m \in A_{ij,t}} M\,(m) \sqrt{v_{i,t} v_{j,t}}\, e^{-d_{ij}/\lambda} / f_{ij}, \quad \lambda = 600 \quad (5)$$

where $w_{ij,t}$ is the potential flow on the corridor, in gravity index units; M is the mode multiplier of the layer, and lambda the decay length in kilometres; w_t, used below, is the sum of $w_{ij,t}$ over all corridors. The betweenness coefficient, the anchor mass and the decay length are stated conventions. Each is applied in the same way to every period. Differences between periods are therefore driven only by the dated layers. Section 4.1 varies each convention in turn. Table 1 reports the resulting masses.

Table 1 Topological node masses by period

Node	1948	1970	1990	2010	2025
Bagan	3.53	3.53	3.53	3.62	3.62
Mandalay	18.0	18.0	18.0	18.18	18.18
Bhamo	2.0	2.0	2.0	2.0	2.0
Monywa	2.0	2.0	2.0	2.0	2.0
Yenangyaung	4.63	4.63	4.63	4.63	4.63
Pyay	3.79	3.79	3.79	3.71	3.71
Bago	19.94	19.94	19.94	13.76	13.76
Yangon	29.45	29.45	29.45	33.97	33.97
Pathein	10.81	10.81	10.81	10.81	10.81
Mawlamyine	11.76	11.76	11.76	11.76	11.76
Sittwe	3.75	3.75	3.75	3.75	3.75
Toungoo	8.47	8.47	8.47	5.47	5.47
Muse	4.41	4.41	4.41	4.41	4.41
Myawaddy	4.41	4.41	4.41	4.41	4.41
Naypyidaw	8.21	8.21	8.21	11.06	11.06
Kunming	12.0	12.0	12.0	12.0	12.0
Bangkok	12.0	12.0	12.0	12.0	12.0
Sea	12.0	12.0	12.0	12.0	12.0

Source: Authors' calculations.

3.3 The optimisation objective

Give each node a binary label. The label records which side of a two-way division it falls on. The objective is the weight that crosses the division.

$$C_t(x) = \sum_{i<j} w_{ij,t}\left(x_i + x_j - 2x_i x_j\right) \quad (6)$$

where is the weight crossing the division, in gravity index units; is the binary label of node i; the bracket equals one when the two endpoints differ, and zero otherwise. Maximising this objective is the maximum-cut problem, written in quadratic unconstrained binary form. The economic meaning is direct. The solution divides the eighteen places into two groups. It chooses the division for which the potential flow running between the groups is largest. The line it draws is the boundary of greatest exchange. Neither group is a sector, an industry or a policy region. Both are sets of places. Hence, the solution of equation (6) is the division of the eighteen nodes into two groups such that the total corridor weight running between the groups is as large as possible. It is best described as a maximum-interaction bisection: the divide across which the geography and the technology of the period route the greatest potential flow. Because the objective maximises flow across a line, two places joined by a heavy corridor tend to fall on opposite sides. Readers used to spatial clustering may find this surprising. $C_t(x)x_i$

3.4 Solution by Quantum Approximate Optimization Algorithm

Equation (6) is a quadratic unconstrained binary optimisation problem. Substituting spin variables which take the values plus one and minus one gives the equivalent quadratic form.

$$C_t(z) = \frac{W_t}{2} - H_t(z), \qquad H_t(z) = \sum_{i<j} \frac{w_{ij,t}}{2} z_i z_j \quad (7)$$

where $(z_i = 1 - 2x_i)$ is the spin variable of node i, taking the value plus one or minus one; $H_t(z)$ is the Ising energy of the configuration, in gravity index units; $\frac{w_{ij,t}}{2}$ is a constant offset which does not affect the location of the optimum.

Maximising the cut is therefore identical to minimising the Ising energy, whose ground states encode the optimal partitions (Lucas, 2014). Every optimum is at least doubly degenerate, since exchanging the labels of the two groups leaves the cut unchanged.

Promoting each spin variable in Equation (7) to a Pauli operator acting on one qubit gives the cost Hamiltonian of the quantum formulation.

$$\hat{H}_C = \sum_{i<j} \frac{w_{ij,t}}{2} \hat{Z}_i \hat{Z}_j, \qquad \hat{H}_C \left|x\right\rangle = \left(\frac{W_t}{2} - C_t(x)\right)\left|x\right\rangle \tag{8}$$

Where $\hat{H}_C$ is the cost Hamiltonian, an operator on the state space of eighteen qubits; $\hat{Z}_i$ is the Pauli spin operator acting on qubit i, with eigenvalues plus one and minus one; ($|x\rangle$)is the computational basis state labelled by the binary string x. Equation (8) is a different mathematical object from Equation (6). The first is an operator on a complex vector space of dimension two hundred and sixty-two thousand one hundred and forty-four; the second is a real-valued function on binary strings. They are connected by the eigenvalue relation, and the practical consequence is that minimising the expectation of the Hamiltonian is exactly equivalent to maximising the classical cut. The quantum step introduces no new optimisation problem and no new economics; it is a re-encoding.

The Quantum Approximate Optimization Algorithm prepares a parameterised state by alternating layers of a cost unitary, which is diagonal in the computational basis and compiles to one two-qubit rotation per corridor, with a mixing operator which factorises into single-qubit rotations, acting on the uniform superposition over all partitions.

$$\left|\psi(\boldsymbol{\gamma}, \boldsymbol{\beta})\right\rangle = \prod_{l=1}^{p} e^{-i\beta_l \hat{B}}\ e^{-i\gamma_l \hat{H}_C}\ H^{\otimes n} \left|0\right\rangle^{\otimes n} \tag{9}$$

where $|\psi\rangle$ is the variational state prepared by the circuit; p is the circuit depth, the number of alternating layers; $\boldsymbol{\gamma}$ and $\boldsymbol{\beta}$ are the two variational parameters of layer one; B is the mixing operator, the sum of Pauli X operators over all qubits; $|+\rangle^{\otimes n}$ is the uniform superposition over all binary strings, prepared by one Hadamard gate per qubit. The quantity the classical outer loop minimises is the expectation of the cost in the prepared state, equivalently the negative of the expected cut.

$$\mathbb{E}[C] = \sum_{x \in \{0,1\}^n} |a_x|^2\ C_t(x) \tag{10}$$

where $\mathbb{E}[C]$ is the expected cut of the prepared state, in gravity index units; a_x is the complex amplitude of basis state x in the prepared state; the squared modulus of a_x is the probability of observing x on measurement. One scaling property is used in implementation. Multiplying all weights by a constant rescales the landscape so that an instance can be solved on weights normalised by their maximum and scored in the original units, which keeps the informative range of the phase parameter of order one regardless of the size of the weights.

3.5 Robustness by classical enumeration

Five quantities in the model are set by convention and then varied. They are the distance decay length, the terrain friction divisor, the mode multiplier ladder, the betweenness coefficient and the external anchor mass. Each one is varied in turn, and for every alternative setting the exact classical optimum is computed again from the beginning. The robustness check is therefore a full re-solution, not a re-estimation or a standard error. All divisions are enumerated again for each setting and for each of the five periods, which gives a new exact optimum every time. Three things are then compared against the baseline: which cities fall on each side of the division, whether that division is the same in all five periods, and how far the optimum rises between 1948 and 2025. A setting is reported as passing only when the division itself is unchanged. Section 4.1 summarises the five conventions.

With eighteen binary variables, there are 262,144 possible labellings. Once the relabelling of the two groups is removed, 131,072 distinct divisions remain. Every instance in this paper is enumerated in full. The optimum is therefore exact, not approximate. Enumeration takes a fraction of a second per period. The same objective can be written as the ground state of an Ising cost Hamiltonian. It can then be given to a variational quantum algorithm. That formulation is implemented here. Appendix D reports it strictly as a

methodological benchmark. At this problem size exact enumeration is immediate, so no claim of quantum advantage is made. Appendix B gives the simulator settings. The pipeline is written in Python, using NumPy and SciPy only. It implements its own geodesic solver, betweenness routine, enumerator and state-vector simulator.

4. Results and Discussion

4.1 A fixed spatial divide, 1948 to 2025

Table 2 Exact optimum by period, with total weight and the uncut residual

Period	Corridors	W	C*	C*/W	W - C*
1948	22	998.26	936.35	0.938	61.91
1970	22	998.26	936.35	0.938	61.91
1990	22	1034.26	972.35	0.9401	61.91
2010	23	1267.65	1202.67	0.9487	64.98
2025	23	1267.65	1202.67	0.9487	64.98

Source: Authors' calculations.

The ratio of the optimum to total weight sits between 0.938 and 0.949 in every period. That level carries no information. Appendix Table C5 sets it against two hundred random networks drawn on the same eighteen nodes, with the same number of corridors and the same weights, each solved exactly. The observed ratio lies inside that null. What the model identifies is therefore the membership of the two groups, reported in Table 3, and the corridors that cross between them, reported in Table 7. It is not the level of the cut.

The best division is the same in all five periods. It is unique in each. Seventy-seven years of infrastructure never moved it. Group A holds the maritime anchor, both border gates, the administrative capital and the river and delta feeder towns. Group B holds the two primate cities, both land anchors, and the coastal and dry-zone secondary centres. Each border gate falls on the opposite side from the market it serves. This is the signature of an objective that maximises flow across a line. It is not what a method that groups places by similarity would produce.

Table 3 The best division, with degree, betweenness and mass in 2025

Node	Group	Type	Degree	Betweenness	Mass
Bagan	A	city	2	0.0515	3.62
Mandalay	B	city	5	0.5074	18.18
Bhamo	A	city	1	0.0	2.0
Monywa	A	city	1	0.0	2.0
Yenangyaung	B	city	2	0.0074	4.63
Pyay	A	city	2	0.0588	3.71
Bago	A	city	3	0.3235	13.76
Yangon	B	city	6	0.3971	33.97
Pathein	A	city	3	0.1103	10.81
Mawlamyine	B	city	4	0.2206	11.76
Sittwe	B	city	2	0.0	3.75
Toungoo	B	city	2	0.2059	5.47
Muse	A	city	2	0.1176	4.41
Myawaddy	A	city	2	0.1176	4.41
Naypyidaw	A	city	3	0.4412	11.06
Kunming	B	anchor	1	0.0	12.0
Bangkok	B	anchor	1	0.0	12.0
Sea	A	anchor	4	0.0	12.0

Source: Authors' calculations.

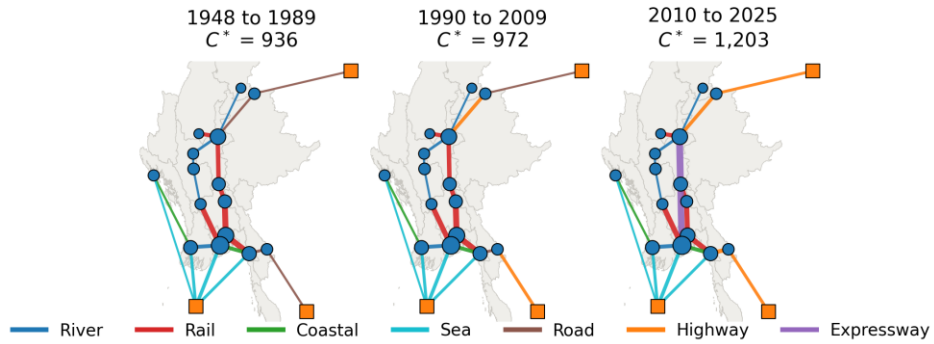

Note: Corridor width rises with the square root of gravity weight, on a scale shared by the three panels. Circles are trade centres and squares are external market anchors, sized by node mass. Node names are given in Figure 3.
Source: Authors' calculations.
Figure 2. The three infrastructure regimes of 1948 to 2025.

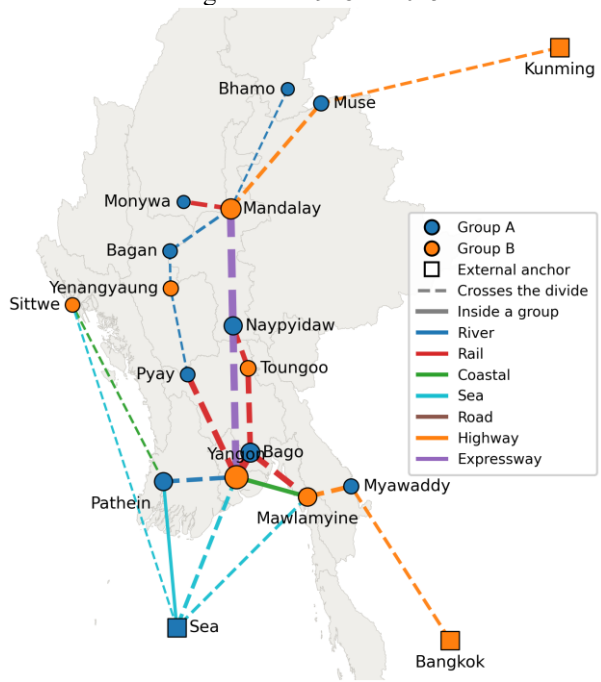

Note: The division is the same in all five periods, so one panel represents them all. The 2010 to 2025 corridor set is drawn. Node color shows group membership and line color shows corridor mode. Squares mark external anchors.
Source: Authors' calculations on geoBoundaries administrative geometry (Runfola et al., 2020), licensed CC BY 4.0.
Figure 3. The best division of the network.

The division is not an artefact of the modelling choices. Table 4 varies each of the five quantities the model fixes by convention. Twelve runs sit behind the five rows, and each run is crossed with all five periods. The decay length varies between 400 and 800 kilometres. The friction divisor varies between 5 and 20, and friction is also removed entirely. The mode multiplier ladder is flattened, compressed and steepened. The betweenness coefficient varies between zero and eight. The anchor mass varies between 6

and 24. The run-by-run matrix is Appendix Table C2, which adds two further settings outside these five conventions.

The best division is identical to the baseline in fourteen of the fifteen. In those fourteen it is also the same across all five periods. There is one exception, and it is reported here rather than set aside. Giving every transport mode the same multiplier changes the division and breaks the invariance across periods. That setting makes a river, a railway and an expressway equivalent. It therefore deletes the very distinction the paper exists to measure, which is why the result is what it is. The honest summary is that the division survives every setting except the one that removes the mechanism under study.

Table 4 The five model conventions, each varied in turn

convention varied	settings tested	runs	C star 2025 range	gain percent range	division unchanged
Distance decay length	400 and 800 km (baseline 600)	2	1024.4 to 1307.5	24.6 to 30.5	Yes
Terrain friction divisor	5 and 20, and friction removed (baseline 10)	3	1058.9 to 1465.7	25.1 to 35.7	Yes
Mode multiplier ladder	flattened, compressed and steepened	3	1274.7 to 1551.5	7.1 to 56.2	Yes, except the flat ladder
Betweenness coefficient	0 and 8 (baseline 4)	2	577.0 to 1804.2	25.4 to 40.5	Yes
External anchor mass	6 and 24 (baseline 12)	2	1173.2 to 1244.3	28.1 to 28.9	Yes

Note: Ranges run across the settings tested in each row. The baseline gives C* of 1,202.7 in 2025 and a gain of 28.4 per cent. Only the flat mode ladder changes the division.
Source: Authors' calculations.

The gain column in the ladder row needs a word, because it is the widest figure in the table. Flattening the ladder gives a rise of 7.1 per cent. Steepening it gives 56.2 per cent. Those two are the extremes of the whole exercise. The reason is simple. The ladder is what separates a river from an expressway, so it governs how much a new layer can add. It does not govern when the additions happen, or which corridors receive them. Section 4.2 reports both of those, and both are stable across every setting tested.

One of those settings deserves its own report, because a reviewer of an earlier version asked about it. Removing the mode multiplier from the cost metric changes the masses but not the outcome. The two mass vectors correlate at 0.9921. The best division is unchanged. The capacity gain moves from 28.4 to 31.3 per cent. The largest single movement is Bago, whose mass falls by 3.17 index units, and the node-level comparison is Appendix Table C3.

Table 5 The mode multiplier removed from the travel cost used for betweenness

Specification	C*, 1948	C*, 2025	Gain, per cent	Mass correlation	Partition as baseline
Baseline: multiplier in cost and in weight	936.3	1202.7	28.4	1.0	Yes
Multiplier removed from the travel cost	853.1	1120.4	31.3	0.9921	Yes

Source: Authors' calculations.

A stronger test uses observed trade. The three anchors carry a fixed mass of twelve by convention. That convention can be replaced with Myanmar's recorded trade shares, taken from the International Merchandise Trade Statistics of the International Monetary Fund (2025). Those shares move a great deal. In 1948 China accounted for 5.1 per cent of Myanmar's trade and Thailand for 0.2 per cent. By 2025 the figures are 34.9 and 14.5 per cent. Setting the anchor masses from those shares, period by period, makes the Kunming mass range from 0.75 to 12.58. That is a factor of seventeen. Table 6 reports the result. The best division is unchanged in all five periods.

Table 6 Anchor masses set from recorded trade shares, period by period

Period	Kunming mass	Bangkok mass	Sea mass	C*	change vs baseline percent	Partition as baseline
1948	1.82	0.07	34.11	964.19	3.0	Yes
1970	0.75	0.0	35.25	964.41	3.0	Yes
1990	5.72	2.3	27.99	987.16	1.5	Yes
2010	3.71	11.07	21.22	1212.97	0.9	Yes
2025	12.58	5.22	18.2	1208.83	0.5	Yes

Note: Trade shares are exports free on board plus imports cost insurance freight, Myanmar as reporter. The shares enter only as this check. They are never an input to the model.
Source: Authors' calculations.

This matters for interpretation. Myanmar's external orientation turned around completely over the period. In 1948 India, the United Kingdom and Sri Lanka took 78 per cent of its trade. By 2025 China and Thailand are the two largest partners. The internal division of the network did not move while that turn took place. Who Myanmar trades with changed. Where geography routes the densest potential exchange did not.

4.2 Integrative expansion with local bypass effects

Capacity is not fixed. The best cut stands at 936.35 index units in 1948 and again in 1970. The 1990 border-highway layer lifts it by 3.8 per cent to 972.35. The 2010 layer lifts it by a further 23.7 per cent to 1,202.67, where it stays in 2025. The total rise is 28.4 per cent in the baseline. Across the settings tested it ranges from 7.1 to 56.2 per cent, and from 15.3 to 56.2 per cent once the flat ladder is set aside. The range rather than the point estimate is the figure to report, for the reason given in Section 4.1. Cities, terrain and functional forms are held fixed, so the rises belong to the named layers.

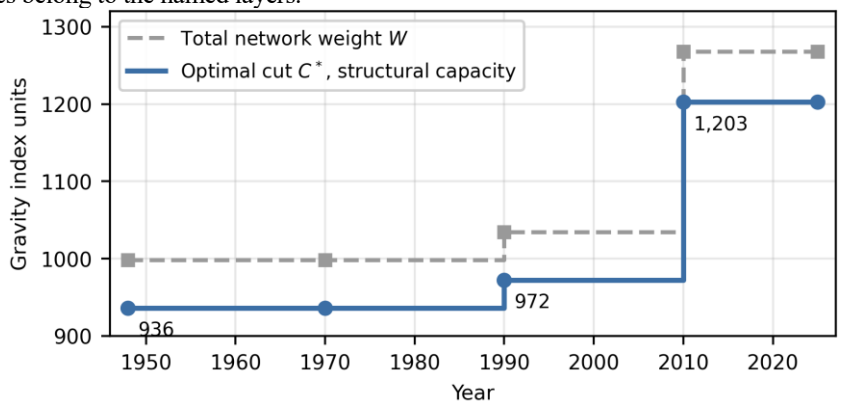

Note: Both series are step functions with exactly three levels. Markers show the five modelled years.
Source: Authors' calculations.
Figure 4. Structural capacity and total network weight, 1948 to 2025.

Where that capacity went is sharper than how much of it there was. In every period exactly two corridors fail to cross the divide. They are the coastal link from Mawlamyine to Yangon and the sea link from Pathein to the maritime anchor. The weight held inside the groups is 61.91 index units in 1948, 1970 and 1990. It rises only to 64.98 in 2010 and 2025.

The two layers together add 269.39 index units of network weight. Of that, 266.32 units fall on corridors that cross the divide. That is 98.9 per cent. Measured this way the investment of those two decades was integrative rather than internal. It added capacity between the two groups rather than within either.

Table 7 Corridors that do not cross the best division, by period

Period	Corridor	Weight
1948	Mawlamyine - Yangon	41.49
1948	Pathein - Sea	20.42
1970	Mawlamyine - Yangon	41.49
1970	Pathein - Sea	20.42
1990	Mawlamyine - Yangon	41.49
1990	Pathein - Sea	20.42
2010	Mawlamyine - Yangon	44.56
2010	Pathein - Sea	20.42
2025	Mawlamyine - Yangon	44.56
2025	Pathein - Sea	20.42

Source: Authors' calculations.

Investment that was integrative nationally was redistributive locally. The 2010 expressway demotes the towns of the old trunk road. Bago falls from 19.94 to 13.76 index units of mass. Toungoo falls from 8.47 to 5.47. Each loses roughly a third. Yangon rises from 29.45 to 33.97 and Naypyidaw from 8.21 to 11.06. The model registers the bypass through betweenness alone, with no assumption about traffic. One dateable investment re-ranks the interior hierarchy. The model isolates the effect because nothing else changes between the two periods.

4.3 Structural capacity against realised outcomes

The capacity computed above is a normative object. It describes what the map and the technology of a period make possible. Setting it beside realised outcomes needs care, and two limits are decisive.

The first is that the model holds no realised trade quantity. It therefore cannot identify a gap between potential and realised trade, and cannot price the consequences of any policy. No claim of that kind is made here. The second is that capacity takes only three values over seventy-seven years, while output moves by a factor above thirty. Any ratio of the two is close to a rescaled output series.

What can be compared is the direction of movement. An annual index of real gross domestic product for 1948 to 2025 is assembled for this purpose. Official national accounts growth rates (Myint, 2008) are chained with the World Economic Outlook series of the International Monetary Fund (2025). The series is then split by a search over segment means, with a minimum segment of five years. The number of breaks is chosen by the Bayesian information criterion. The criterion selects two breaks, at 1991 and 2019. Those dates are close to the political turning points usually cited, but not identical to them. A different estimator moves them by a year or two. The three-segment structure is therefore the finding, and the dates are treated as estimator sensitive.

Table 8 Mean annual real growth by estimated segment

Segment	Years	Mean growth, per cent
1948-1991	44	3.15
1992-2019	28	8.53
2020-2025	6	-3.17

Source: Authors' calculations.

Table 9 Flow-weighted effective friction and mean real growth by period window

Period	Window	Effective friction	C*	Mean growth, per cent
1948	1948-1961	0.1772	936.3	3.69
1970	1962-1988	0.1772	936.3	3.0
1990	1989-2009	0.171	972.3	8.55
2010	2010-2019	0.1494	1202.7	6.5
2025	2020-2025	0.1494	1202.7	-3.17

Note: Effective friction is the flow-weighted mean of friction divided by the best available mode multiplier. A lower value means an easier network.
Source: Authors' calculations.

The last window settles the comparison. Between 2020 and 2025 the network carries the lowest effective friction in the whole record, at 0.1494. The same window records the only negative mean growth in the record, at minus 3.17 per cent a year. Physical friction and realised growth are therefore separate. The period in which the country's transport geography was easiest to cross is the period in which its economy did worst. A model built only from geography and infrastructure cannot explain that sign. No attempt is made here to do so. The observation marks a boundary of the approach rather than a result within it. A divide that does not shift in seventy-seven years has a direct implication for planning. Infrastructure raises how much a structure can carry. It does not reorient the structure. Every layer added between 1948 and 2025 changed the capacity of the network. None changed which places exchange across the main divide.

Planning that expects a corridor programme to reorganise the spatial economy is assuming something this record does not support. Planning that treats corridors as raising capacity on a fixed geography is consistent with it. The composition result refines this. Of the capacity added between 1990 and 2010, 98.9 per cent fell on corridors crossing the divide. The programme of those decades is therefore best described as integrative. It deepened exchange between the two groups rather than within either. That is a favourable description at the national scale. It is a cautionary one locally, because the same investment removed about a third of the network weight of the towns it bypassed. What the model does not license must be said plainly. It is a structural benchmark of physical potential. It holds no realised trade. Earlier versions of this work read the gap between flat potential and realised outcomes as a cost of autarky. That reading is withdrawn. No such quantity is identified here. The separation reported in Section 4.3 shows that the binding constraints in the most recent window lie outside anything the model measures.

5. Limitations

Four limitations bound the claims. The first concerns node representation. A single coordinate stands for each city, port and border crossing. That cannot fully represent a large urban area, a port with several terminals, or a border zone with several gates. Corridors are also drawn as straight geodesics rather than routed paths, so terrain is sampled along a straight line rather than along the road as built. The second concerns the external anchors. They are a modelling device. Their number, position and mass are conventions. Section 4.1

and Appendix C show that the division does not depend on them. The capacity level does. The third concerns scale. Eighteen nodes and twenty-three corridors are a curated network, not a gazetteer. The result is conditional on that selection. A denser network would test whether the division survives disaggregation. The fourth matters most for the final period. The 2025 network evaluates surviving physical infrastructure. That is distinct from whether routes can actually be used. Conditions after 2021 may have affected usability without removing any corridor from the ground. Appendix C quantifies what such a divergence would mean. Closing the northern land gate removes 15.7 per cent of 2025 structural capacity. Closing both land gates removes 33.1 per cent. The 2025 row throughout this paper should be read as physical capacity only.

6. Conclusion and Recommendations

This paper used no economic archive at all. Its inputs were coordinates, measured terrain, dated infrastructure and a gravity and topology model, solved by exact enumeration. It has shown that the long-run spatial structure of an economy can be reconstructed where trade records do not survive.

For Myanmar between 1948 and 2025 three results stand. The best division of the trade network is the same in every period, across every convention of the model but one, and under anchor masses set from observed trade shares. Capacity rose about 28 per cent in two dated steps, almost entirely on corridors linking the two groups. And the period with the least physical friction in the record is the period with the weakest growth. The method needs inputs that exist for any country and any period, so it carries to other settings where archives have not survived.

Three implications follow. Each is stated with the caution the evidence supports. The model holds no project costs and makes no cost comparison, so no specific investment is recommended. Firstly, transport capacity is not the binding constraint. The window with the lowest network friction in the record is also the window with the weakest growth. Returns to corridor investment therefore depend on conditions that are not physical. Border facilitation, regulatory predictability and reliable operating conditions matter alongside road capacity. Secondly, bypass effects deserve explicit mitigation. The towns bypassed by the 2010 expressway lost about a third of their network weight. Where such investment goes ahead, support for the secondary centres it bypasses is worth planning alongside it rather than afterwards. Thirdly, gateway diversification is supported by the closure results. The corridor from Mandalay to Muse is the most rugged link in the network. It is also worth 15.7 per cent of 2025 capacity on its own. The two land gates are only partial substitutes. Closing both costs 33.1 per cent of capacity, which is less than the sum of the separate losses but far more than either. Keeping alternatives across the Chinese, Thai and maritime routes reduces exposure to the loss of any one.

For future studies, a routed rather than geodesic corridor geometry would sharpen the friction term. A finer node set built from administrative units would test whether the division survives disaggregation. That second extension would also take the problem past the size at which enumeration is possible, which is the point at which the encoding examined in Appendix D would begin to earn its place.

References

Aschauer, D. A. (1989). Is public expenditure productive? Journal of Monetary Economics, 23(2), 177-200.

Asian Development Bank. (2018). Review of configuration of the Greater Mekong Subregion economic corridors. Asian Development Bank.

Banerjee, A., Duflo, E., & Qian, N. (2020). On the road: Access to transportation infrastructure and economic growth in China. Journal of Development Economics, 145, 102442.

Brandes, U. (2001). A faster algorithm for betweenness centrality. Journal of Mathematical Sociology, 25(2), 163-177.

Brown, I. (2013). Burma's economy in the twentieth century. Cambridge University Press.

Donaldson, D. (2018). Railroads of the Raj: Estimating the impact of transportation infrastructure. American Economic Review, 108(4-5), 899-934.

Donaldson, D., & Hornbeck, R. (2016). Railroads and American economic growth: A market access approach. Quarterly Journal of Economics, 131(2), 799-858.

Farr, T. G., Rosen, P. A., Caro, E., Crippen, R., Duren, R., Hensley, S., Kobrick, M., Paller, M., Rodriguez, E., Roth, L., Seal, D., Shaffer, S., Shimada, J., Umland, J., Werner, M., Oskin, M., Burbank, D., & Alsdorf, D. (2007). The Shuttle Radar Topography Mission. Reviews of Geophysics, 45(2), RG2004.

Findlay, R. (1962). Capital theory and development planning. The Review of Economic Studies, 29(2), 85-98.

Freeman, L. C. (1977). A set of measures of centrality based on betweenness. Sociometry, 40(1), 35-41.

Gallup, J. L., Sachs, J. D., & Mellinger, A. D. (1999). Geography and economic development. International Regional Science Review, 22(2), 179-232.

Hansen, W. G. (1959). How accessibility shapes land use. Journal of the American Institute of Planners, 25(2), 73-76.

International Monetary Fund. (2025). International merchandise trade statistics and World Economic Outlook database. International Monetary Fund.

Ishida, M. (Ed.). (2013). Border economies in the Greater Mekong Subregion. Palgrave Macmillan.

Krongkaew, M. (2004). The development of the Greater Mekong Subregion: Real promise or false hope? Journal of Asian Economics, 15(5), 977-998.

Limao, N., & Venables, A. J. (2001). Infrastructure, geographical disadvantage, transport costs, and trade. World Bank Economic Review, 15(3), 451-479.

Lucas, A. (2014). Ising formulations of many NP problems. Frontiers in Physics, 2, 5.

Myint, U. (2008). Myanmar economy: A comparative view. In M. Skidmore & T. Wilson (Eds.), Dictatorship, disorder and decline in Myanmar. ANU E Press.

Peschel, K. (1985). Spatial structures in international trade: An analysis of long term developments. Papers of the Regional Science Association, 58, 97-111.

Powell, M. J. D. (1994). A direct search optimization method that models the objective and constraint functions by linear interpolation. In S. Gomez & J.-P. Hennart (Eds.), Advances in optimization and numerical analysis (pp. 51-67). Kluwer Academic.

Redding, S. J., & Turner, M. A. (2015). Transportation costs and the spatial organization of economic activity. In G. Duranton, J. V. Henderson, & W. C. Strange (Eds.), Handbook of regional and urban economics (Vol. 5, pp. 1339-1398). Elsevier.

Rodrigue, J.-P. (2020). The geography of transport systems (5th ed.). Routledge.

Runfola, D., Anderson, A., Baier, H., Crittenden, M., Dowker, E., Fuhrig, S., Goodman, S., Grimsley, G., Layko, R., Melville, G., Mulder, M., Oberman, R., Panganiban, J., Peck, A., Seitz, L., Shea, S., Slevin, H., Youngerman, R., & Hobbs, L. (2020). geoBoundaries: A global database of political administrative boundaries. PLOS ONE, 15(4), e0231866.

Tinbergen, J. (1962). Shaping the world economy: Suggestions for an international economic policy. Twentieth Century Fund.

Appendix A. Geospatial Data Registers

These registers record what each coordinate denotes. They also record the basis on which each corridor and its dates are included. No economic quantity appears in any of them.

Table A1. Node register, with the meaning of each coordinate

Node	Modern name	Latitude	Longitude	Type	Arable	Oil	Harbour	the coordinate represents
Bagan	Bagan	21.172	94.860	city	0	0	0	Middle Irrawaddy dry-zone river town
Mandalay	Mandalay	21.975	96.083	city	0	0	0	Head of the central dry zone; junction of river, rail and the road to Yunnan
Bhamo	Bhamo	24.252	97.233	city	0	0	0	Practical head of Irrawaddy navigation
Monywa	Monywa	22.108	95.135	city	0	0	0	Chindwin valley entry point
Yenangyaung	Yenangyaung	20.459	94.873	city	0	1	0	Onshore oil geology (earth-oil seeps of the Irrawaddy embayment)
Pyay	Pyay (Prome)	18.817	95.217	city	0	0	0	Irrawaddy river port at the delta margin
Bago	Bago (Pegu)	17.335	96.481	city	1	0	0	Flat alluvial lower Sittang/Bago plain
Yangon	Yangon (Rangoon)	16.866	96.195	city	1	0	1	Delta alluvium; sheltered estuarine harbor
Pathein	Pathein (Bassein)	16.779	94.732	city	1	0	1	Western delta alluvium; river harbor
Mawlamyine	Mawlamyine (Moulmein)	16.491	97.626	city	0	0	1	Thanlwin estuary harbor
Sittwe	Sittwe (Akyab)	20.146	92.898	city	0	0	1	Kaladan estuary

Node	Modern name	Latitude	Longitude	Type	Arable	Oil	Harbour	the coordinate represents
								harbor
Toungoo	Taungoo	18.940	96.433	city	0	0	0	Sittang valley corridor town
Muse	Muse	23.985	97.904	city	0	0	0	Shweli river crossing on the China frontier
Myawaddy	Myawaddy	16.689	98.508	city	0	0	0	Moei river crossing on the Thai frontier
Naypyidaw	Naypyidaw (Pyinmana)	19.745	96.130	city	0	0	0	Sittang valley rail junction (Pyinmana) ; capital from 2005
Kunming	Kunming (external anchor)	25.043	102.706	anchor	0	0	0	External market anchor: Yunnan / China
Bangkok	Bangkok (external anchor)	13.756	100.502	anchor	0	0	0	External market anchor: Thailand / mainland SE Asia
Sea	Indian Ocean sea lanes (external anchor)	14.000	95.000	anchor	0	0	0	External market anchor: maritime world trade via the Bay of Bengal

Note: Endowment flags take the value one when the condition is present. The factor multiplies 1.5 for arable delta or alluvial land, 1.5 for onshore oil geology and 1.25 for a natural harbour.
Source: Authors' calculations.

Table A2. Corridor register: dated technology layers

From	To	Mode	From	Until	Documented basis
Bhamo	Mandalay	river	1948	-	Upper Irrawaddy navigation
Mandalay	Bagan	river	1948	-	Middle Irrawaddy
Bagan	Yenangyaung	river	1948	-	Middle Irrawaddy
Yenangyaung	Pyay	river	1948	-	Middle Irrawaddy
Pyay	Yangon	river	1948	-	Lower Irrawaddy / delta channels
Monywa	Mandalay	river	1948	-	Chindwin junction traffic
Yangon	Bago	river	1948	-	Bago river and delta creeks
Yangon	Pathein	river	1948	-	Delta waterways
Yangon	Mawlamyine	coastal	1948	-	Gulf of Martaban coastal shipping
Pathein	Sittwe	coastal	1948	-	Bay of Bengal coastal shipping
Yangon	Pyay	rail	1948	-	Line of 1877 (inherited)
Yangon	Bago	rail	1948	-	Line of 1885 (inherited)
Bago	Toungoo	rail	1948	-	Line of 1885 (inherited)
Toungoo	Naypyidaw	rail	1948	-	Mainline via Pyinmana (1889, inherited)
Naypyidaw	Mandalay	rail	1948	-	Mainline via Pyinmana (1889, inherited)
Mandalay	Monywa	rail	1948	-	Sagaing-Monywa branch (inherited)
Bago	Mawlamyine	rail	1948	-	Martaban line with ferry; Thanlwin rail bridge from 2005
Bago	Toungoo	road	1948	-	NH1 Sittang valley road
Mandalay	Muse	road	1948	1989	Burma Road (1938) via Lashio, unimproved
Mandalay	Muse	highway	1990	-	Mandalay-Lashio-Muse road rebuilt as the Union highway to the border gate
Muse	Kunming	road	1948	2009	Burma Road continuation into Yunnan
Muse	Kunming	highway	2010	-	Chinese expressway network reaches Ruili/Muse in the 2000s
Mawlamyine	Myawaddy	road	1948	2009	Kawkareik pass road, single-lane over the Dawna Range
Mawlamyine	Myawaddy	highway	2010	-	Asian Highway AH1; Kawkareik bypass completed 2015
Myawaddy	Bangkok	road	1948	1989	Route to the Thai rail/road head at Mae Sot
Myawaddy	Bangkok	highway	1990	-	Thai national highway network to Mae Sot / Bangkok
Yangon	Naypyidaw	expressway	2010	-	Yangon-Naypyidaw Expressway (2009-2010)
Naypyidaw	Mandalay	expressway	2010	-	Naypyidaw-Mandalay Expressway
Yangon	Sea	sea	1948	-	Yangon river outlet to open sea lanes
Pathein	Sea	sea	1948	-	Pathein river outlet to the Bay of Bengal
Mawlamyine	Sea	sea	1948	-	Thanlwin estuary to the Gulf of Martaban
Sittwe	Sea	sea	1948	-	Kaladan estuary to the Bay of Bengal

Note: A blank closing year means the layer is still active in 2025. Several rows may describe the same physical corridor at different dates. The inherited river and rail network follows the historical

account in Brown (2013). The border-highway and expressway upgrades of 1990 and 2010 follow the Greater Mekong Subregion corridor literature (Krongkaew, 2004; Ishida, 2013; Asian Development Bank, 2018).
Source: Compiled by the authors from the Greater Mekong Subregion corridor literature (Krongkaew, 2004; Ishida, 2013; Asian Development Bank, 2018) and the historical accounts in Brown (2013) and Myint (2008).

Table A3. Corridor geometry and measured terrain friction, ordered by ruggedness

Corridor	Geodesic, km	Ruggedness, m/km	Friction f
Mandalay - Muse	290.53	11.39	2.139
Kunming - Muse	500.53	10.58	2.058
Bhamo - Mandalay	278.32	9.95	1.995
Bangkok - Myawaddy	388.86	9.69	1.969
Mandalay - Monywa	98.97	4.3	1.43
Mawlamyine - Myawaddy	96.64	4.29	1.429
Bagan - Yenangyaung	78.95	4.17	1.417
Mandalay - Naypyidaw	246.94	3.55	1.355
Pyay - Yenangyaung	185.32	2.93	1.293
Bagan - Mandalay	154.75	1.92	1.192
Naypyidaw - Yangon	318.73	1.36	1.136
Pathein - Sittwe	420.0	1.27	1.127
Bago - Toungoo	177.72	1.18	1.118
Bago - Yangon	60.17	0.91	1.091
Naypyidaw - Toungoo	94.63	0.89	1.089
Pyay - Yangon	239.53	0.68	1.068
Bago - Mawlamyine	153.63	0.4	1.04
Mawlamyine - Yangon	158.18	0.34	1.034
Pathein - Yangon	156.23	0.13	1.013
Mawlamyine - Sea	394.38	0.0	1.0
Pathein - Sea	308.85	0.0	1.0
Sea - Sittwe	716.0	0.0	1.0
Sea - Yangon	342.08	0.0	1.0

Source: Authors' calculations.

Table A4. Every corridor in every period, with weight and crossing status

Period	Corridor	Weight	Crosses divide
1948	Bagan - Mandalay	15.5	Yes
1948	Bagan - Yenangyaung	7.51	Yes
1948	Bago - Mawlamyine	114.01	Yes
1948	Bago - Toungoo	121.03	Yes
1948	Bago - Yangon	261.2	Yes
1948	Bangkok - Myawaddy	7.73	Yes
1948	Bhamo - Mandalay	5.67	Yes
1948	Kunming - Muse	6.14	Yes
1948	Mandalay - Monywa	46.25	Yes
1948	Mandalay - Muse	10.27	Yes
1948	Mandalay - Naypyidaw	59.43	Yes
1948	Mawlamyine - Myawaddy	17.17	Yes
1948	Mawlamyine - Sea	18.47	Yes
1948	Mawlamyine - Yangon	41.49	No

1948	Naypyidaw - Toungoo	65.39	Yes
1948	Pathein - Sea	20.42	No
1948	Pathein - Sittwe	8.42	Yes
1948	Pathein - Yangon	40.72	Yes
1948	Pyay - Yangon	86.31	Yes
1948	Pyay - Yenangyaung	7.14	Yes
1948	Sea - Sittwe	6.1	Yes
1948	Sea - Yangon	31.89	Yes
1970	Bagan - Mandalay	15.5	Yes
1970	Bagan - Yenangyaung	7.51	Yes
1970	Bago - Mawlamyine	114.01	Yes
1970	Bago - Toungoo	121.03	Yes
1970	Bago - Yangon	261.2	Yes
1970	Bangkok - Myawaddy	7.73	Yes
1970	Bhamo - Mandalay	5.67	Yes
1970	Kunming - Muse	6.14	Yes
1970	Mandalay - Monywa	46.25	Yes
1970	Mandalay - Muse	10.27	Yes
1970	Mandalay - Naypyidaw	59.43	Yes
1970	Mawlamyine - Myawaddy	17.17	Yes
1970	Mawlamyine - Sea	18.47	Yes
1970	Mawlamyine - Yangon	41.49	No
1970	Naypyidaw - Toungoo	65.39	Yes
1970	Pathein - Sea	20.42	No
1970	Pathein - Sittwe	8.42	Yes
1970	Pathein - Yangon	40.72	Yes
1970	Pyay - Yangon	86.31	Yes
1970	Pyay - Yenangyaung	7.14	Yes
1970	Sea - Sittwe	6.1	Yes
1970	Sea - Yangon	31.89	Yes
1990	Bagan - Mandalay	15.5	Yes
1990	Bagan - Yenangyaung	7.51	Yes
1990	Bago - Mawlamyine	114.01	Yes
1990	Bago - Toungoo	121.03	Yes
1990	Bago - Yangon	261.2	Yes
1990	Bangkok - Myawaddy	23.19	Yes
1990	Bhamo - Mandalay	5.67	Yes
1990	Kunming - Muse	6.14	Yes
1990	Mandalay - Monywa	46.25	Yes
1990	Mandalay - Muse	30.8	Yes
1990	Mandalay - Naypyidaw	59.43	Yes
1990	Mawlamyine - Myawaddy	17.17	Yes
1990	Mawlamyine - Sea	18.47	Yes
1990	Mawlamyine - Yangon	41.49	No
1990	Naypyidaw - Toungoo	65.39	Yes
1990	Pathein - Sea	20.42	No
1990	Pathein - Sittwe	8.42	Yes
1990	Pathein - Yangon	40.72	Yes
1990	Pyay - Yangon	86.31	Yes
1990	Pyay - Yenangyaung	7.14	Yes
1990	Sea - Sittwe	6.1	Yes
1990	Sea - Yangon	31.89	Yes
2010	Bagan - Mandalay	15.77	Yes

2010	Bagan - Yenangyaung	7.6	Yes
2010	Bago - Mawlamyine	94.72	Yes
2010	Bago - Toungoo	80.81	Yes
2010	Bago - Yangon	233.08	Yes
2010	Bangkok - Myawaddy	23.19	Yes
2010	Bhamo - Mandalay	5.7	Yes
2010	Kunming - Muse	18.42	Yes
2010	Mandalay - Monywa	46.48	Yes
2010	Mandalay - Muse	30.96	Yes
2010	Mandalay - Naypyidaw	173.33	Yes
2010	Mawlamyine - Myawaddy	51.5	Yes
2010	Mawlamyine - Sea	18.47	Yes
2010	Mawlamyine - Yangon	44.56	No
2010	Naypyidaw - Toungoo	61.0	Yes
2010	Naypyidaw - Yangon	150.46	Yes
2010	Pathein - Sea	20.42	No
2010	Pathein - Sittwe	8.42	Yes
2010	Pathein - Yangon	43.74	Yes
2010	Pyay - Yangon	91.62	Yes
2010	Pyay - Yenangyaung	7.06	Yes
2010	Sea - Sittwe	6.1	Yes
2010	Sea - Yangon	34.25	Yes
2025	Bagan - Mandalay	15.77	Yes
2025	Bagan - Yenangyaung	7.6	Yes
2025	Bago - Mawlamyine	94.72	Yes
2025	Bago - Toungoo	80.81	Yes
2025	Bago - Yangon	233.08	Yes
2025	Bangkok - Myawaddy	23.19	Yes
2025	Bhamo - Mandalay	5.7	Yes
2025	Kunming - Muse	18.42	Yes
2025	Mandalay - Monywa	46.48	Yes
2025	Mandalay - Muse	30.96	Yes
2025	Mandalay - Naypyidaw	173.33	Yes
2025	Mawlamyine - Myawaddy	51.5	Yes
2025	Mawlamyine - Sea	18.47	Yes
2025	Mawlamyine - Yangon	44.56	No
2025	Naypyidaw - Toungoo	61.0	Yes
2025	Naypyidaw - Yangon	150.46	Yes
2025	Pathein - Sea	20.42	No
2025	Pathein - Sittwe	8.42	Yes
2025	Pathein - Yangon	43.74	Yes
2025	Pyay - Yangon	91.62	Yes
2025	Pyay - Yenangyaung	7.06	Yes
2025	Sea - Sittwe	6.1	Yes
2025	Sea - Yangon	34.25	Yes

Source: Authors' calculations.

Appendix B. Optimization Simulator setting

Simulator settings are as follows. The expectation of the cut is evaluated exactly from the state vector, so the objective carries no sampling noise. Parameters are optimized by the Constrained Optimization by Linear Approximation method (Powell, 1994), from three random restarts of one hundred iterations. Measurement statistics are drawn separately, as 8,192 shots from the optimized state. Circuit quality and sampling luck are therefore reported as separate quantities. The problem is solved on weights normalized by the largest corridor weight, which rescales the phase parameter without changing the landscape. Every random element is seeded.

Tables B1 and B2 work a three-node instance completely through both paths. The instance is drawn from the 2025 network, so the arithmetic can be checked by hand.

Table B1. Complete enumeration of a three-node instance, classical and Ising forms

State	x(Yangon)	x(Bago)	x(Mawlamyine)	Corridors cut	C(x)	H(z)
|000>	0	0	0	none	0.0	186.1783
|001>	0	0	1	BM, MY	139.2792	46.8991
|010>	0	1	0	BY, BM	327.7962	-141.6179
|011>	0	1	1	BY, MY	277.6378	-91.4595
|100>	1	0	0	BY, MY	277.6378	-91.4595
|101>	1	0	1	BY, BM	327.7962	-141.6179
|110>	1	1	0	BM, MY	139.2792	46.8991
|111>	1	1	1	none	0.0	186.1783

Note: The nodes are Yangon, Bago and Mawlamyine, with masses 33.9706, 13.7647 and 11.7647. Corridor weights are 233.0774, 94.7188 and 44.5604. Total weight is 372.3566. The optimum is 327.7962 and isolates Bago from the other two.
Source: Authors' calculations.

Table B2. Amplitudes and measurement probabilities of the depth-one circuit

State	Eigenvalue of H	After Hadamard	final amplitude	Probability	Cut
|000>	186.1783	0.35355	+0.00784 -0.07108i	0.00511	0.0
|001>	46.8991	0.35355	-0.13336 +0.14822i	0.03976	139.28
|010>	-141.6179	0.35355	-0.47731 +0.18607i	0.26245	327.8
|011>	-91.4595	0.35355	-0.38477 +0.21126i	0.19268	277.64
|100>	-91.4595	0.35355	-0.38477 +0.21126i	0.19268	277.64
|101>	-141.6179	0.35355	-0.47731 +0.18607i	0.26245	327.8
|110>	46.8991	0.35355	-0.13336 +0.14822i	0.03976	139.28
|111>	186.1783	0.35355	+0.00784 -0.07108i	0.00511	0.0

Note: At the grid optimum the phase parameter is 0.00543 and the mixing parameter 1.2043. There the expected cut is 290.1253, or 88.51 per cent of the optimum. The probability mass on the two exactly optimal assignments is 0.5249, against 0.2500 for uniform guessing.
Source: Authors' calculations.

Appendix C. Robustness and Sensitivity Matrices

Every variant below is solved by exact enumeration. Nothing here depends on a heuristic or on the variational circuit. Divisions are compared with the baseline after allowing for the relabelling of the two groups.

Table C1. Myanmar's recorded trade shares with China, Thailand and India

Period	China percent	Thailand percent	India percent	rest of world percent	total trade million usd
1948	5.1	0.2	37.5	94.7	364
1970	2.1	0.0	11.4	97.9	258
1990	15.9	6.4	4.2	77.7	1076
2010	10.3	30.7	9.4	58.9	11866
2025	34.9	14.5	4.5	50.6	29372

Note: Exports free on board plus imports cost insurance freight, Myanmar as reporter, from the International Merchandise Trade Statistics of the International Monetary Fund (2025). These shares are used only to set the anchor masses in Table 8. They are never an input to the model.
Source: Authors' calculations.

Table C2. The sensitivity grid run by run, fifteen settings

Specification	C*, 1948	C*, 2025	Gain, per cent	Period-invariant	Partition as baseline
baseline	936.3	1202.7	28.4	Yes	Yes
distance decay 400 km	822.3	1024.4	24.6	Yes	Yes
distance decay 800 km	1001.9	1307.5	30.5	Yes	Yes
friction 1 + r/5	846.7	1058.9	25.1	Yes	Yes
friction 1 + r/20	997.1	1309.3	31.3	Yes	Yes
friction removed	1080.1	1465.7	35.7	Yes	Yes
mode ladder flat, all modes 8	1190.6	1274.7	7.1	No	No
mode ladder steep	993.3	1551.5	56.2	Yes	Yes
mode ladder compressed	1107.1	1276.3	15.3	Yes	Yes
betweenness coefficient 0	410.6	577.0	40.5	Yes	Yes
betweenness coefficient 8	1439.2	1804.2	25.4	Yes	Yes
endowment removed	717.0	959.6	33.8	Yes	Yes
anchor mass 6	915.7	1173.2	28.1	Yes	Yes
anchor mass 24	965.5	1244.3	28.9	Yes	Yes
technology out of cost metric	853.1	1120.4	31.3	Yes	Yes

Note: The twelve runs summarised in the main text, plus two settings outside the five conventions: the endowment factor switched off, and the technology multiplier removed from the cost metric. The flat ladder is the only setting in which the division changes. It assigns every mode the same multiplier, which removes the technology differentiation the study measures.
Source: Authors' calculations.

Table C3. Node masses with and without the mode multiplier in the travel cost, 2025 network

Node	Baseline mass	mass without multiplier in cost	Difference
Bago	13.76	10.59	-3.18
Yenangyaung	4.63	6.35	1.72
Naypyidaw	11.06	9.53	-1.53
Mandalay	18.18	16.76	-1.41
Pyay	3.71	4.41	0.71
Bagan	3.62	4.06	0.44
Yangon	33.97	33.58	-0.39
Toungoo	5.47	5.12	-0.35
Bhamo	2.0	2.0	0.0
Monywa	2.0	2.0	0.0
Pathein	10.81	10.81	0.0
Mawlamyine	11.76	11.76	0.0
Sittwe	3.75	3.75	0.0
Muse	4.41	4.41	0.0
Myawaddy	4.41	4.41	0.0
Kunming	12.0	12.0	0.0
Bangkok	12.0	12.0	0.0
Sea	12.0	12.0	0.0

Note: Ordered by the size of the difference. Nine of the eighteen nodes are unaffected. The two vectors correlate at 0.9921 and the best division is the same under both.
Source: Authors' calculations.

Table C4. Maritime anchor displacement and removal, and corridor closure scenarios

Scenario	C*, 1948	C*, 2025	Change, per cent	Period-invariant	Partition as baseline
maritime anchor moved -2, -2	914.8	1180.2	29.0	Yes	Yes
maritime anchor moved +2, +2	951.8	1226.9	28.9	Yes	Yes
maritime anchor removed	823.8	1094.1	32.8	Yes	Yes
northern gate closed	-	1013.5	-15.7	-	No
eastern gate closed	-	954.5	-20.6	-	No
both land gates closed	-	804.8	-33.1	-	No

Note: The first three rows move or remove the maritime anchor. The division of the remaining nodes does not change. The closure rows delete corridors from the 2025 network. There the division does change, which is why the 2025 result is reported as physical capacity only.
Source: Authors' calculations.

Table C5. Near-bipartiteness of the corridor network against a null of comparable random networks

Statistic	Value
observed C*/W, 2025	0.9487
null mean	0.9525
null 5th percentile	0.9043
null 95th percentile	0.9895
random networks drawn	200

Note: Two hundred random networks were drawn on the same eighteen nodes, with the same number of corridors and the same weights, and each was solved exactly. The observed ratio of optimum to total weight lies inside that null. The level of the ratio is therefore reported only for completeness, and

no inference is drawn from it. The informative outputs are group membership and the set of crossing corridors.
Source: Authors' calculations.

Appendix D. Algorithmic Performance and Baselines

This subsection reports how well the two solution methods solve the problem. It carries no economic content. It is included because an approximation ratio means nothing without reference points.

Table D1. Exact solution and classical heuristics, as ratios to the optimum

Period	Exact optimum	Random	Greedy	Local search, mean	Local search, hit rate
1948	936.35	0.5292	0.9289	0.9726	0.615
1970	936.35	0.5321	0.9289	0.9733	0.625
1990	972.35	0.5325	0.9315	0.9659	0.405
2010	1202.67	0.5269	1.0	1.0	1.0
2025	1202.67	0.5264	1.0	1.0	1.0

Source: Authors' calculations.

Complete enumeration takes a fraction of a second per period and is exact. A uniformly random division already reaches about 53 per cent of the optimum. That follows from two facts. A random cut has expected value of half the total weight, and the optimum is near 0.94 of total weight. Greedy construction reaches between 92.9 and 100 per cent. Multi-start local search recovers the exact optimum from a large share of random starts, and from every start in the last two periods.

Table D2. The quantum benchmark on the 2025 network, at depths one to three

Depth p	Parameters	Expected cut	Expected ratio	P(optimum)	Best-sampled ratio	seconds
1	2	847.51	0.7047	0.000128	0.9953	36.3
2	4	900.34	0.7486	0.000228	0.9953	65.7
3	6	972.24	0.8084	0.00149	1.0	101.4

Note: The expected ratio is computed exactly from the optimised state vector. It is a property of the circuit. The best-sampled ratio is the best of 8,192 measurements. It is a property of the shot budget.
Source: Authors' calculations.

Two numbers must be kept apart. The expected ratio of the circuit rises with depth, from 0.7047 at depth one to 0.8084 at depth three. It stays below the greedy construction at every depth tested. The best-sampled ratio is much higher. That is because 8,192 draws from a distribution with a small but real mass on the optimum will usually find it. The chance that any single shot returns an optimum is about one in several thousand.

A further question concerns the last two periods. The 2010 and 2025 corridor networks are identical by construction. No corridor opens, closes or is upgraded between them. Any difference in their reported quantum results is therefore optimiser and sampling noise, not an effect of period. Table D3 demonstrates both halves of that statement. Solving the two networks from the same six seeds returns identical values in every case. Solving the same network from different seeds does not.

Table D3. The identical 2010 and 2025 networks solved from six seeds each

Seed	expected ratio 2010	expected ratio 2025	P(optimum)	Best-sampled ratio	results identical
101	0.7599	0.7599	0.000589	1.0	Yes
202	0.7615	0.7615	0.000549	1.0	Yes
303	0.7772	0.7772	0.000526	1.0	Yes
404	0.7779	0.7779	0.000577	1.0	Yes
505	0.7779	0.7779	0.000574	1.0	Yes
606	0.7779	0.7779	0.000578	1.0	Yes

Note: Each run uses depth two, three restarts and one hundred iterations, as in the rest of the paper. The two period columns agree exactly, because the two networks are the same problem. The spread across seeds is the size of the noise that would otherwise be mistaken for a period effect.
Source: Authors' calculations.

Reporting only the best-sampled figure would overstate the circuit, so both are given. Rising performance with depth is the expected behaviour. It is evidence that the implementation is correct, not evidence about Myanmar. At this problem size the classical methods win, and the quantum formulation is reported on that basis.